Thermal properties and microstructure of gypsum board and its dehydration products : a theoretical and experimental investigation

FIRE AND MATERIALS
Fire Mater. 2012; **36**:575–589
Published online 21 September 2011 in Wiley Online Library (wileyonlinelibrary.com). DOI: 10.1002/fam.1117

Thermal properties and microstructure of gypsum board and its dehydration products: A theoretical and experimental investigation

Q. L. Yu*,† and H. J. H. Brouwers

Department of Architecture, Building and Planning, Eindhoven University of Technology, P. O. Box 513, 5600 MB, Eindhoven, The Netherlands

SUMMARY

This article addresses the thermal properties and the microstructure of gypsum boards produced from β-hemihydrate by studying its dehydration process.

Dehydration reaction of gypsum boards was investigated from both micro and macro levels, employing thermogravimetric analysis and a ventilated oven. A new dehydration mechanism of gypsum was proposed. The thermal properties of gypsum board such as enthalpy of reaction, specific heat capacity, and thermal conductivity were studied by differential scanning calorimetry and a heat transfer analyzer, respectively. The effect of void fraction and dehydration on thermal physical properties of gypsum board was investigated. The microstructure of the gypsum board at high temperature was studied with experiments and modeling. A model was proposed to describe the microstructure of a dehydrated system at high temperature, and experiments indicate its validity. Furthermore, the mechanical properties of gypsum at high temperature were investigated, and the effect of water content was discussed as well. Copyright © 2011 John Wiley & Sons, Ltd.

Received 20 January 2011; Revised 19 April 2011; Accepted 5 June 2011

KEY WORDS: β-hemihydrate; gypsum board; dehydration; thermal properties; microstructure; mechanical properties

List of symbols

ROMAN

h_0 initial mass of the unreacted hemihydrate (g)
s saturation rate pore volume water
w_0 initial mass of the water (g)

GREEK

φ volume fraction
λ thermal conductivity (W/(mK))
v specific volume (cm^3/g)
ω specific molar volume (cm^3/mol)

*Corresponding to: Q. L. Yu, Department of Architecture, Building and Planning, Eindhoven University of Technology, PO Box 513, 5600 MB Eindhoven, The Netherlands.
†E-mail: q.yu@bwk.tue.nl

SUBSCRIPT

a	air
ah	anhydrite
dh	dihydrate
e	effective
f	fluid, can be water or air
hh	hemihydrate
s	solid
v	void fraction
n	nonevaporable
w	capillary water

1. INTRODUCTION

Gypsum plaster was used in Egyptian pyramids at least 4000 years ago [1] and is still extensively applied in building along with other cementitious materials such as cement and lime. Gypsum plasterboard, also called drywall, is widely used for interior walls or ceilings because of its easy fabrication feature, environmental friendliness, good fire resistance, aesthetics, low price, etc. Gypsum plasterboard is made from hemihydrate by hydrating with water. Hemihydrate occurs in two formations, that is, the α and β types, although β-hemihydrate is mainly applied because the hydration product of the α-hemihydrate is too brittle to be used as building material [2].

Gypsum, or $CaSO_4 \cdot 2H_2O$, contains about 20.9% by mass chemically combined water, which is readily lost at an elevated temperature. This phenomenon is called dehydration, and the dehydration mechanism of gypsum has been intensively investigated so far [3–7]. Groves [3] reported that first $CaSO_4 \cdot 0.5H_2O$ and then $CaSO_4$ is formed during gypsum dehydration, which was also confirmed by Kuntze [4] and Paulik *et al*. [5]. The effect of experimental conditions such as temperature, pressure, and particle size of gypsum was investigated as well. The dehydration reaction is endothermic, that is, an amount of energy is needed to break the crystal water [8–10], which also explains why gypsum has a good fire resistance property. Thermal properties such as specific heat and thermal conductivity of gypsum plasterboard were also studied extensively [8–15]. However, the reported thermal properties of gypsum (plasterboard) [8–15] vary with each other considerably because of many possible reasons such as the physical properties of the applied raw material, the composition of the investigated gypsum plasterboard, and the production procedure of the gypsum plasterboard.

The present work aims at a better understanding of the performance of gypsum board at elevated temperatures, from its physical properties such as microstructure, thermal properties, and mechanical properties. A β-hemihydrate produced from the flue gas desulfurization (FGD) gypsum was used in this study as raw material in consideration of sustainability because FGD gypsum is a by-product of the process of desulfurization of combustion gases of fossil fuels (coal, lignite, and oil) in power stations [2]. The thermal behavior of gypsum boards was investigated by means of thermogravimetric analysis (TGA), differential scanning calorimetry (DSC), and thermal conductivity measurements employing a commercial heat transfer analyzer. A new dehydration mechanism was proposed in the present study. The relation between the void fraction of the gypsum board and its thermal conductivity was analyzed. The microstructure of gypsum board beyond dehydration was studied both by modeling and by experiments employing a scanning electron microscope (SEM). A new model was derived to describe the void fraction of dehydrated gypsum board, and it was validated by experiments. Furthermore, the mechanical properties of gypsum at elevated temperatures were studied, and the effect of the water content was investigated as well.

2. MATERIAL AND EXPERIMENTAL

2.1. Material and sample preparation

The applied material, that is, β-hemihydrate, in the present study was provided by Knauf Gips KG (Germany). The β-hemihydrate was produced from the FGD gypsum. The β-hemihydrate was

DOI: 10.1002/fam

characterized in the present study in order to evaluate its physical properties such as mineralogy, element, particle size distribution, and microstructure. X-ray diffraction (XRD) patterns were obtained using a Rigaku diffractometer (Rigaku Co., Tokyo, Japan) operating at room temperature in order to confirm the mineralogy and crystallinity. A chemical analysis of the material was carried out with energy-dispersive X-ray spectroscopy (EDX). The particle size distribution (PSD) was measured with Mastersizer 2000 (Malvern Instruments Ltd., Worcestershire, UK). The microstructure was analyzed with SEM.

The investigated gypsum board in the present study was produced from the applied β-hemihydrate by using a similar method as real gypsum board production [16,17]. An accelerator (a fine gypsum powder) was used to adjust a final setting time of 5–7 min in order to simulate a real gypsum plasterboard production process [17]. The studied sample included powder, prism, and board according to the different objectives with the powder sampled from the prepared prisms or boards.

2.2. Dehydration of gypsum

When heated, gypsum takes two steps of endothermic decomposition reactions [3–5]. When the first dehydration reaction occurs, $CaSO_4{\cdot}2H_2O$ is converted to $CaSO_4{\cdot}0.5H_2O$, which reads as follows:

$$CaSO_4{\cdot}2H_2O + \text{heat} \rightarrow CaSO_4{\cdot}0.5H_2O + 1.5H_2O \quad (1)$$

The second dehydration reaction occurs when $CaSO_4{\cdot}0.5H_2O$ is converted to $CaSO_4$, which reads as follows:

$$CaSO_4{\cdot}0.5H_2O + \text{heat} \rightarrow CaSO_4 + 0.5H_2O \quad (2)$$

However, it is indicated that the thermal properties related to the dehydration reaction such as the dehydration temperature and the required energy are still not certain [3–7]. This can be caused by the physical properties such as the composition and the microstructure of the investigated gypsum. Therefore, in the present study, the dehydration reaction was studied. The dehydration of the gypsum board was investigated from both discrete and continuous heating rates. TGA was applied to study the dehydration reaction from a micro level by employing a simultaneous TGA–DSC test equipment (STA 449 F1 Jupiter®, Netzsch Instruments, Inc., Burlington, MA, USA). The investigated gypsum was sampled from the prepared gypsum boards. A ventilated oven was also applied to study the dehydration reaction from a macro level. The gypsum board was used for the macro level dehydration study. Prior to the tests, all the samples were dried in the oven at 40 °C to a constant mass to remove the free moisture.

2.3. Microstructure of dehydrated system

Figure 1 shows schematically the composition of the hydrated and dehydrating system by volume. The system consists of dihydrate and void before the dehydration, as shown in Figure 1(a). During the dehydration process, as indicated in Eqs. (1) and (2), the chemically combined water in the matrix is gradually released. The dehydrating system is composed of the void space, the dihydrate, and the regenerated hemihydrates, then the anhydrite, as shown in Figures 1(b) and 1(c), respectively. The temperature reaches 200 °C in less than 1 min under real fire test following the standard ISO 834-1 [18]. Therefore, the emphasis here is only focused on the fully dehydrated system in the present study.

The microstructure of the dehydrating system was investigated both by modeling and by experiments, that is, SEM analysis. A model was proposed in the present study to describe the void fraction of the dehydrated system, which was validated by performed experiments. SEM analysis was performed on two gypsum board samples prepared with different initial water contents to study the crystal shape of the particles as well as the void fraction of the system.

The strength of the dehydrated system was also tested on gypsum prisms according to EN 13279-2 [19] to investigate the effect of the microstructural change. The flexural strength was measured with the three-point bending test, and the compressive strength was determined by applying a load to the two broken parts of the specimen obtained from the flexural strength test.

DOI: 10.1002/fam

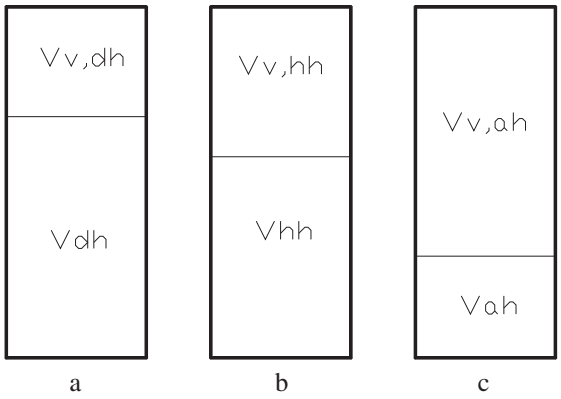

Figure 1. Schematic diagram of the volume composition of the gypsum system. (a) Before dehydration (dihydrate); (b) upon first dehydration step (hemihydrate); and (c) upon second dehydration step (anhydrite).

2.4. Thermal properties of gypsum

To study the thermal behavior of one material such as heat transfer during the fire, obviously the understanding of its thermal physical properties is of vital importance. However, available literature [7–15] demonstrates a wide variation of the thermal properties such as enthalpy, thermal conductivity, and specific heat capacity. Hence, experiments were performed to study the thermal physical properties of the gypsum boards in the present study.

The specific heat capacity of the gypsum was investigated on the format of the board because to date, most of the effort was only put on the powder [7–15]. A commercial heat transfer analyzer (ISOMET 2104, Applied Precision Ltd., Bratislava, Slovakia) was used to measure the volumetric heat capacity of the prepared gypsum board. This heat transfer analyzer could not be operated above 40°C [20], so the following procedure was used to measure the volumetric heat capacity of the gypsum board at high temperature. First, the samples, here the gypsum boards, were heated to the desired temperature for dehydration reaction (here, enough time was used to assure a full dehydration reaction), then the samples were cooled down to room temperature, and finally, the volumetric heat capacity was measured.

The dehydration reaction is endothermic, that is, an amount of heat is needed. The difference between the reported values from the literature [7–15] indicates the effect of the composition and the microstructure of the investigated gypsum. Ghazi Wakili *et al*. [14] also investigated the influence of the heating rate of the employed DSC, and they reported that only at a low heating rate (5°C/min) the peaks of the two dehydration steps (Eqs. (1) and (2)) are clearly distinguishable. The present study measured the energy needed for the dehydration reaction of the used gypsum employing DSC (STA 449 F1 Jupiter®), and the influence of the heating rate was also studied by using two different heating rates of 5 and 20°C/min, respectively.

The thermal conductivity of a material is related with its density and composition, which was for instance investigated by De Korte and Brouwers [21]. However, it is shown that most of the available literature [8–15] only studied one or two types of commercially available gypsum plasterboards without providing composition information, and the effect of water content on thermal conductivity of gypsum board was not reported before. The thermal conductivity of the gypsum board was analyzed in the present study by employing the same heat transfer analyzer (ISOMET 2104). The water content as well as the effect of dehydration was investigated.

3. RESULTS AND DISCUSSION

3.1. Material characterization

The measured XRD results were analyzed by program XPowder, and Figure 2 shows the XRD patterns of the used β-hemihydrate. All the main peaks refer to $CaSO_4 \cdot 0.5H_2O$, which indicates that the material

DOI: 10.1002/fam

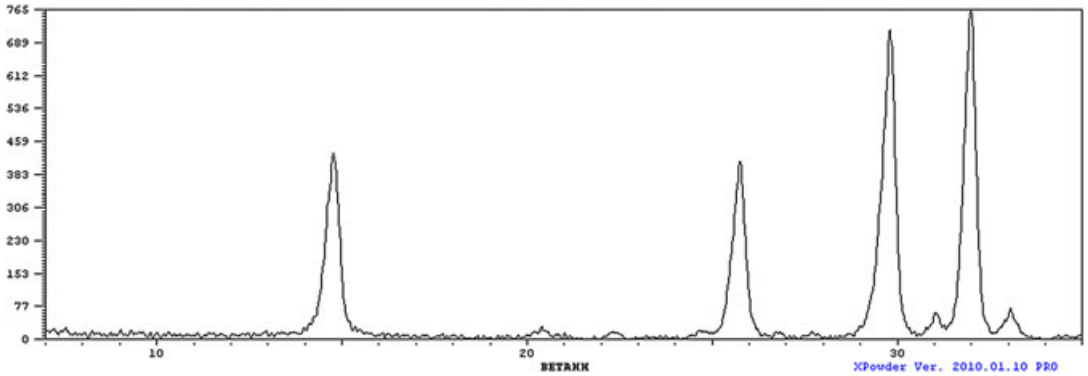

Figure 2. The X-ray diffraction patterns of the β-hemihydrate (all the main peaks point to $CaSO_4 \cdot 0.5H_2O$).

almost entirely consists of $CaSO_4 \cdot 0.5H_2O$. The chemical composition measured by EDX is listed in Table I. It shows that there are only very small impurities (Si, Mg, and Al in total less than 3% by mass) in the sample, which also confirms the XRD result. The measured proportion of Ca and S is in line with the theoretical value (i.e. 1:1 in molar proportion), which indicates that there is no Ca-based impurity in the material. The computed mass content of $CaSO_4 \cdot 0.5H_2O$ is 96.94%, but it should be mentioned that this value may have a very slight error because hydrogen could not be detected during the EDX analysis.

The PSD of the β-hemihydrate was measured by applying a so-called laser diffraction method with a detection range of 0.02–2000 μm [22]. The β-hemihydrate powder was measured in wet mode by dispersing it in a transport liquid, here propan-2-ol because β-hemihydrate is reactive with water. The PSD of the β-hemihydrate is shown in Figure 3. It can be seen that 90% of the particles are finer than 78.30 μm and 50% are finer than 23.49 μm, with the surface weighted mean (D [2,3]) of 6.07 μm. The fine particles contribute to a fast hydration reaction when water is added, which is confirmed by our previous study [23]. The specific surface area was calculated from the measured PSD results based on an assumption that all the particles are spheres [22], yielding 0.377 m^2/g (9877.4 cm^2/cm^3). A detailed calculation description can be found in Refs. [22,24]. The measured Brunner Emmet Teller (BET) surface area of the β-hemihydrate is 7.50 m^2/g. The value is the same as the measured Brunner Emmet Teller external surface area, which indicates that there are no micropores inside. The SEM analysis of the used β-hemihydrate is shown in Figure 4(a). It is clear that the β-hemihydrate is composed of irregularly shaped particles, and their sizes are in line with the PSD measurement.

3.2. Dehydration process analysis

The dehydration of the gypsum board in microscale (the samples were in the range of 40–50 mg) was measured by employing TGA–DSC, and the final heating temperature was set at 1000 °C, considering the possible decomposition of the impurities in the used raw material. Two different heating rates of 20 and 5 °C/min were applied to study the effect of heating rate on the dehydration process. The mass loss during the dehydration of gypsum is shown in Figure 5. TGA results show that under both heating rates, the sample starts losing weight at around 80 °C, but the mass becomes constant at different temperatures of 270 °C (20 °C/min) and 180 °C (5 °C/min), respectively, which indicates a completion of the dehydration reaction. It is demonstrated that the heating rate does not affect the dehydration

Table I. Chemical composition analyzed by energy-dispersive X-ray spectroscopy.

Element	wt.%	at.%	K ratio
O	48.86	67.84	0.0714
Mg	0.87	0.80	0.0030
Al	0.80	0.66	0.0037
Si	1.32	1.05	0.0082
S	21.46	14.87	0.1758
Ca	26.68	14.79	0.2285
Total	100.00	100.00	

DOI: 10.1002/fam

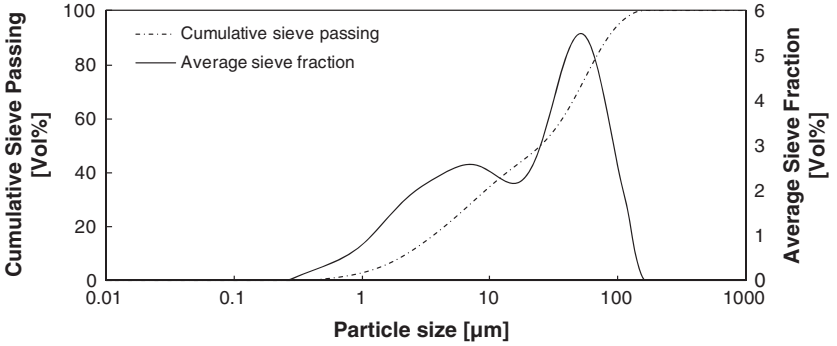

Figure 3. The particle size distribution of the β-hemihydrate.

commencing temperature, but it influences its ending temperature, which indicates that the energy needed for the dehydration is related not only to the temperature but also to the heating duration. Mehaffey *et al*. [8] reported that all chemically combined water was released between 100 and 160°C, and Ghazi Wakili and Hugi [15] reported a temperature range of about 150 to 300°C by using the same heating rate of 20°C/min. As can be seen, the values considerably differ from each other. This probably can be explained from the microstructure of the investigated gypsum, which indicates its effect on the thermal behavior of gypsum board. The derivative curve of the mass loss in Figure 5 shows that two steps of dehydration reaction occur, which is in line with literature [3–7]; however, it is also clear that these two steps are not distinguishable in case of a higher heating rate test (i.e. 20°C/min).

There is another mass loss from about 620°C until around 800°C. According to the chemical analysis results listed in Table I, the molar amounts of Ca and S are the same, which indicates that there is no impurity of $CaCO_3$ in the used material. From the decomposition temperature of about 600°C and the chemical element analysis as listed in Table I, it can be concluded that the impurity is $MgCO_3$, and the decomposition reaction reads as follows:

$$MgCO_3 \rightarrow MgO + CO_2 \tag{3}$$

This finding is different from that of Ghazi Wakili *et al*. [14] who considered the second mass loss as the decomposition of the $CaCO_3$, based on the fact that the $CaCO_3$ decomposes in this temperature range too [25]. Mehaffey *et al*. [8] also reported a mass loss at around 650°C, but they did not analyze the possible reason.

The mass loss of the samples at macroscale during the heating using the ventilated oven is shown in Figure 6(a). Here, the samples were heated with a discrete order, that is, first, the temperature was fixed at one value and the samples were heated until a constant mass (here, the constant mass means the mass remains the same with a measurement interval of 24 h), then the temperature was raised to another value and the samples were heated again until a constant mass, and so on. The tests were performed two times with the same experimental conditions. The excellent agreement between the results from the two batches indicates the reliability of the results. Results show no mass loss occurred at 55°C, and then the dehydration reaction took place from 80 to 120°C. The very small mass loss between 120 and 220°C (less than 1%) indicates the completion of the water release. The average mass loss is in good agreement with the mass loss measured with the TGA from both continuous and discrete heating methods. The mass loss of gypsum board measured from the TGA with discrete order is shown in Figure 6(b). The heating order (the sample was first heated to 80°C at 20°C/min, and then the temperature was kept at 80°C for 4 h; next, the temperature was increased to 120°C at 20°C/min and kept for 3 h; then, the temperature was increased to 150°C and kept for 1 h; and finally, the temperature was increased to 300°C) is the same as the test performed in macro level, as shown in Figure 6(b). It is obvious that these two results are in line with each other, which indicates that the isothermal time is enough for the total water release within that period. These findings indicate that given sufficient

DOI: 10.1002/fam

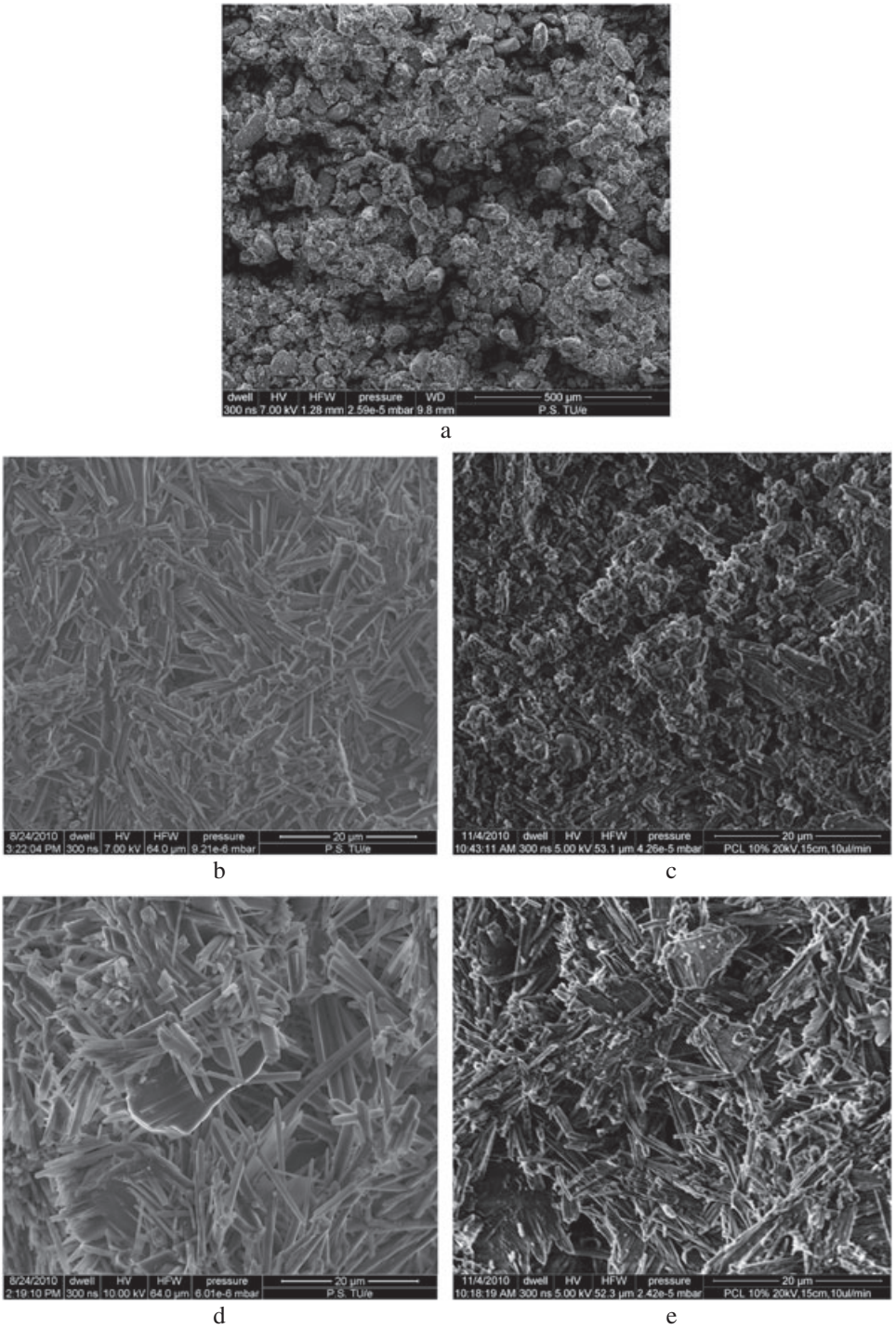

Figure 4. The scanning electron microscope picture of the gypsum system. (a) β-Hemihydrate; (b) gypsum board (w_0/h_0=0.65); (c) dehydrated gypsum board (w_0/h_0=0.65); (d) gypsum board (w_0/h_0=0.80); and (e) dehydrated gypsum board (w_0/h_0=0.80).

heating time, gypsum board produced from β-hemihydrate can accomplish the first step dehydration (i.e. a release of 1.5 molecules of crystal water, Eq. (1)) at 80°C and a total dehydration (i.e. a release of two molecules of crystal water, Eq. (2)) at 120°C. To the authors' knowledge, this has never been reported before.

DOI: 10.1002/fam

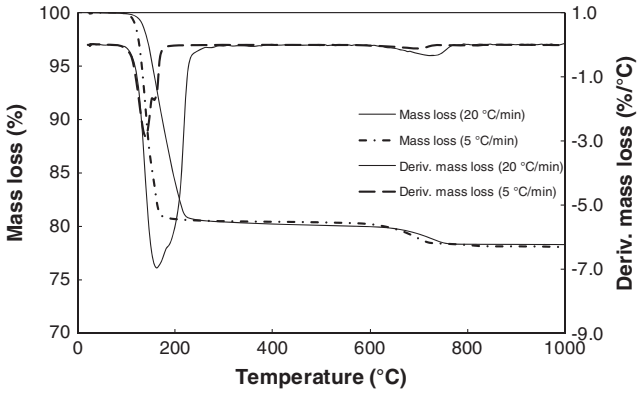

Figure 5. The thermogravimetric analysis results of the samples from gypsum boards (heating rates: 20 and 5°C/min).

3.3. *Microstructure and related mechanical properties*

As illustrated by Eqs. (1) and (2), hemihydrate and then anhydrite is generated from dihydrate during the dehydration reaction. Therefore, the volume composition of the fully dehydrated system consists of only anhydrite and void fraction, that is, air, as shown in Figure 1(c). During the dehydration process, the molar amount of $CaSO_4$ remains constant; therefore, the following expression is obtained

$$\frac{\varphi_{ah}}{\omega_{ah}} = \frac{\varphi_{dh}}{\omega_{dh}} \tag{4}$$

with φ as the volume fraction and ω as the specific molar volume (cm^3/mol).

Under the assumption that the volume of the system remains constant during the dehydration, Eq. (4) becomes

$$\varphi_{ah} = \frac{\varphi_{dh}}{\omega_{dh}} \times \omega_{ah} = \left(1 - \varphi_{v,dh}\right) \times \frac{\omega_{ah}}{\omega_{dh}} \tag{5}$$

and hence,

$$\varphi_{v,ah} = 1 - \varphi_{ah} = 1 - \left(1 - \varphi_{v,dh}\right) \times \frac{\omega_{ah}}{\omega_{dh}} \tag{6}$$

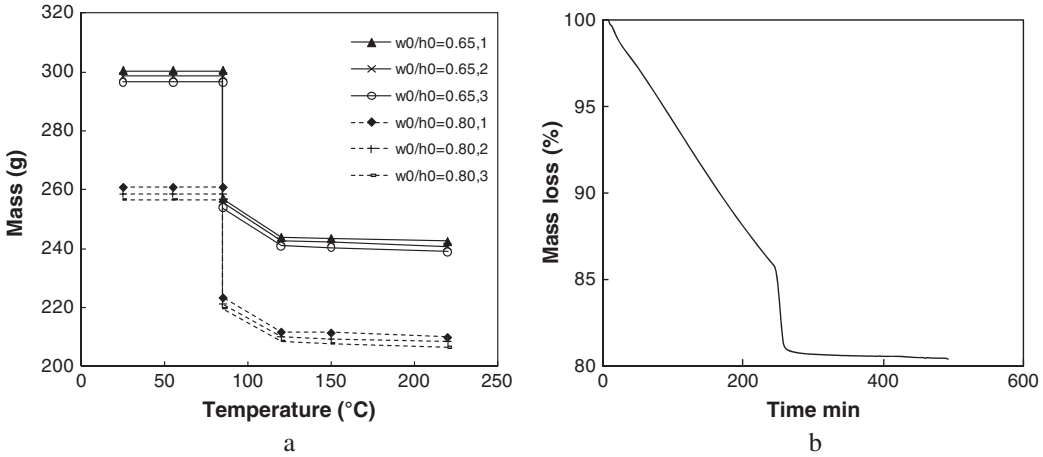

a b

Figure 6. The mass loss of the gypsum boards measured with discrete heating order. (a) Heated with a ventilated oven (6 specimens) and (b) heated with TGA.

DOI: 10.1002/fam

Substituting the void fraction model for gypsum as proposed by Brouwers [26] and Yu and Brouwers [23] in case of full hydration yields

$$\varphi_{v,ah} = 1 - \varphi_{ah} = 1 - \left(1 - \varphi_{v,dh}\right) \times \frac{\omega_{ah}}{\omega_{dh}} = 1 - \left(1 - \frac{\frac{w_0}{h_0} - \frac{v_n}{v_w}\frac{w_n}{h}}{\frac{v_h}{v_w} + \frac{w_0}{h_0}}\right) \times \frac{\omega_{ah}}{\omega_{dh}} \quad (7)$$

Substituting the values for β-hemihydrate from Table II into Eq. (7), $\varphi_{v,ah}$ is obtained as follows:

$$\varphi_{v,ah} = \frac{0.01 + \frac{w_0}{h_0}}{0.38 + \frac{w_0}{h_0}} \quad (8)$$

Eq. (8) gives the relation between the void fraction of the dehydrated system and the initial water/hemihydrate (w_0/h_0) of the gypsum board. In the present study, experiments were carried out with different w_0/h_0 to study the void fraction of the system beyond dehydration. The results are shown in Figure 7. The good agreement between the proposed model (Eq. (8)) and the measured values (from both the literature [8,11,14,15] and own performed experiments) indicates the validity of this microstructural model.

Values from the literature [8,11,14,15] were calculated from the following method. First, the initial water/hemihydrate ratios were assessed using the given density values and the void fraction expression for gypsum (dihydrate) [23,26], assuming no impurities (Table IV). Next, the void fraction of the gypsum board after dehydration was calculated on the basis of the relation between the given density and the density of the pure anhydrite (Table II), assuming no impurities as well. Because of the assumption of no impurities in the gypsum board, there are some errors in the calculated values, which are also included in Figure 7. As can be seen, the calculated values from the literature [8,11,14,15] are a little bit smaller than the model predictions but still in line with the model presented here.

The microstructure of the dehydrated system was also investigated by SEM, and the results are shown in Figure 4. Figures 4(b) and 4(d) show the SEMs of the gypsum boards prepared with different initial water/hemihydrate ratios of 0.65 and 0.80, respectively. It is obvious that the gypsum crystals are regularly formed prisms, and the porosity of the gypsum with a w_0/h_0 of 0.65 in Figure 4(b) is clearly lower than that of the gypsum in Figure 4(d). However, after the dehydration reaction, or after the anhydrite was produced, the microstructure of the system changed considerably from regularly shaped prisms to irregularly broken particles or tubes (Figures 4(c) and 4(e)). This indicates a reduced bonding between the crystals. Also, it is clear from the SEM pictures that the void fraction increased after dehydration indeed.

The strength loss of the samples produced with different w_0/h_0 beyond dehydration is shown in Figure 8. The strength (both the compressive and flexural strengths) decreased more than 75% after dehydration in both gypsum boards prepared from an initial w_0/h_0 of 0.65 and 0.80. Results show that the strength of the gypsum with an initially higher void fraction decreased more than that of gypsum with a lower void fraction. These findings indicate evidently that the matrix of the gypsum with a higher void fraction becomes weaker compared with that of the gypsum with a lower void fraction. They also indicate that the strength of the gypsum depends on the bonding between the crystals, and the water release of the gypsum has a bigger influence when it has a higher void fraction.

Table II. Parameters of the microstructure model [26].

Substance	M (g/mole)	ρ (g/cm^3)	ω (cm^3/mole)	v_h/v_w	w_n/h	v_n/v_w	$v_n w_n/v_w h$	v_s/v_h
Anhydrite	136.14	2.58	52.77					
β-Hemihydrate	145.15	2.62	55.40	0.38	0.186	0.71	0.13	0.054
α-Hemihydrate	145.15	2.76	52.59	0.36	0.186	0.81	0.15	0.035
Dihydrate	172.18	2.32	74.22	0.43	–	–	–	–

DOI: 10.1002/fam

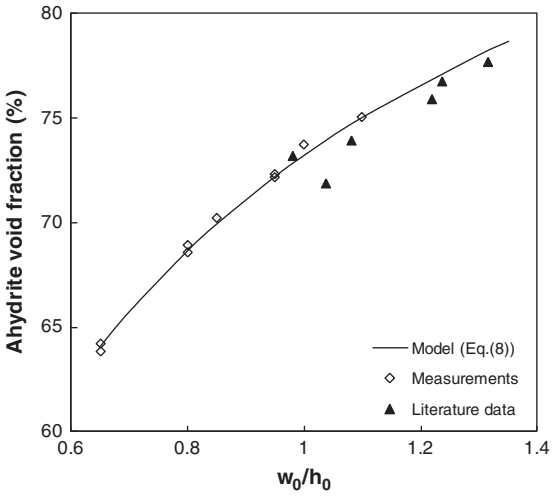

Figure 7. The void faction of the dehydrated gypsum boards versus the water–hemihydrate ratio (w_0/h_0) (experimental data taken from own tests and Refs. [8,11,14,15]).

3.4. Thermal properties analysis

Figure 9 shows the measured DSC results of the gypsum board. The energy needed for the dehydration reaction, that is, the integrated surface area underneath the peak, is calculated by the DSC system, yielding 500kJ/kg under the heating rate of 20°C/min and 515kJ/kg under the heating rate of 5°C/min, respectively. These values are in line with those of Mehaffey *et al*. [8] and Ghazi Wakili *et al*. [14], who reported a value of 500 and 450kJ/kg, respectively. However, this is questionable, because the investigated gypsum in the present study has a quite different purity (~96.9% in Table I) (69.5% and 81% in Refs. [8] and [14], respectively), whereas according to Mehaffey *et al*. [8], the energy was only calculated based on the composition. This finding indicates that the energy needed for the dehydration is related not only with the composition, that is, purity of the gypsum, but also strongly with the microstructure.

The present study also investigated the influence of the heating rate on the dehydration reaction, as shown in Figure 9. The energy needed with different heating rates is in line with each other. This means that the heat needed for the dehydration is independent of the employed heating rate. However, it is different from Ghazi Wakili *et al*. [14] who reported that two clearly distinguishable peaks were found when applying a lower heating rate of 5°C/min. In the present study, the peaks are similar under different heating rates, as shown in Figure 9. The difference is that the peak values are different under different heating rates, which is in line with those of Mehaffey *et al*. [8].

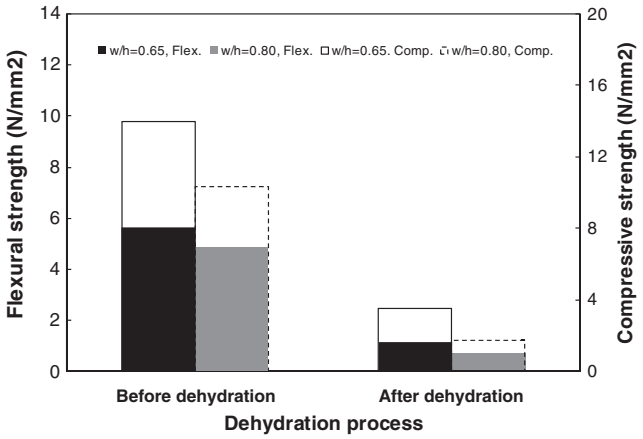

Figure 8. The strength of the gypsum boards versus the void fraction (before and after dehydration).

DOI: 10.1002/fam

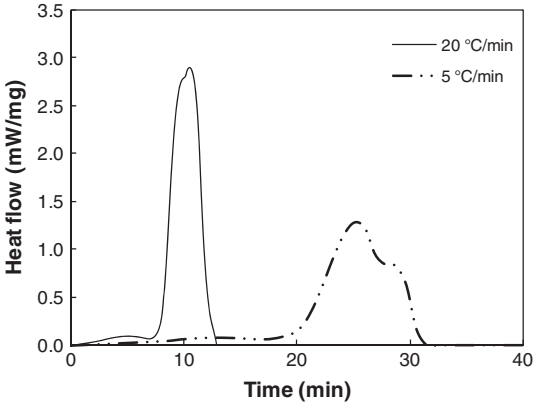

Figure 9. The measured differential scanning calorimetry result of the gypsum boards.

The measured volumetric heat capacity of gypsum board prepared with different water contents is listed in Table III. It is clear that the calculated specific heat based on the mass of different samples is in line with each other, which also confirms the validity of the volumetric specific capacity measurement. The calculated specific heat of gypsum here (1355 J/(kg K) in average) is higher than that of Mehaffey *et al*. [8], who reported a value of 950 J/(kg K) under room temperature. This might be caused by the difference of the composition and the microstructure between the two applied materials.

The volumetric specific capacity of the gypsum boards decreased after the dehydration reaction, as shown in Table III. The specific heat capacity based on the mass of the dehydrated system was calculated, yielding 787 J/(kg K) in average. The lower value of the heat capacity of the dehydrated system compared with the gypsum board also indicates the reduction of the bonding between the anhydrite crystals, which also confirms the microstructure analysis in the previous section.

The measured thermal conductivity of the investigated gypsum board prepared with different water contents is listed in Table III. As can be seen, thermal conductivity is strongly related to the density or the porosity of the gypsum board. The thermal conductivity increases with an increase of the density. Zehner and Schlunder [27] proposed an expression to describe the relation between the thermal conductivity and the porosity with consideration of the particle shape as follows:

$$\lambda_e = \lambda_f\left(1-\sqrt{1-\varphi_v}\right)+\lambda_f\sqrt{1-\varphi_v}\cdot A \tag{9}$$

where

$$\begin{aligned} A &= \frac{2}{N}\left(\frac{B}{N^2}\frac{k-1}{k}\ln\left(\frac{k}{B}\right)-\frac{B+1}{2}-\frac{B-1}{N}\right),\ N=1-\frac{B}{k};\\ B &= C\left(\frac{1-\varphi_v}{\varphi_v}\right)^{10/9},\ k=\frac{\lambda_s}{\lambda_f} \end{aligned} \tag{10}$$

Table III. The measured thermal physical properties of gypsum boards (density, volumetric heat capacity, and thermal conductivity).

Mix (w_0/h_0)	Density (g/cm^3)		Volumetric heat capacity (J/(m^{3}K))		Thermal conductivity (W/(mK))	
Conditions	Room temperature	After dehydration	Room temperature	After dehydration	Room temperature	After dehydration
0.65	1.112	0.895	1.54×10^6	0.72×10^6	0.359	0.159
0.7	1.084	0.872	1.50×10^6	0.68×10^6	0.346	0.138
0.85	0.956	0.768	1.20×10^6	0.59×10^6	0.276	0.111
1.0	0.845	0.678	0.96×10^6	0.54×10^6	0.238	0.106

DOI: 10.1002/fam

Here, the parameter C is the shape factor [27] and λ_s and λ_f are the thermal conductivities of solid and fluid (here, the fluid can be either water or air), respectively.

The model from Zehner and Schlunder [27] considered that the system is composed of two phases, but normally, gypsum boards absorb a little amount of free water from the ambient conditions during the storage. Somerton *et al*. [28] proposed an equation for porous medium filled by a mixture of two fluids (in the present study, i.e. air and free moisture) as follows:

$$\lambda_e = \lambda_{e,a} + \sqrt{s}\cdot\left(\lambda_{e,w} - \lambda_{e,a}\right) \tag{11}$$

Here, $\lambda_{e,a}$ and $\lambda_{e,w}$ are computed from Eqs. (9) and (10), using the thermal conductivity values of air and water, respectively.

In the present study, the effect of the void fraction on the thermal conductivity was investigated considering the system is composed of three phases, that is, solid, water, and air and the effect of the particle shape factor. This is processed by combining the two models from Zehner and Schlunder [27] and Somerton *et al*. [28]. At ambient conditions, a water saturation of 3% (i.e. s in Eq. (11)) was used here because it was found that in average (with different void fractions), a water content of 1.5% by mass of the gypsum board is adsorbed during the cooling/storage time. Incorporating Eqs. (9) and (10) into Eq. (11), the parameters (λ_s and C) were obtained by optimization, employing the 'Solver' tool from Microsoft Excel and the experimental data (Tables III and IV), yielding 1.55 W/(m K) (λ_s) and 2.75 (C) for pure gypsum, respectively. The results are listed in Table V. The derived thermal conductivity value for pure dihydrate is in line with that of Horai and Simmons [29] who gave a value of 1.26 W/(m K). The obtained value for the shape factor of gypsum is in line with that of Zehner and Schlunder [27] who reported a shape factor value of 2.50 for cylinder and tubes. This is also confirmed by the SEM analysis as shown in Figures 4(c) and 4(e).

Then, the thermal conductivity calculated from the model by substituting the optimized parameters (C and λ_s) and the experimental data (Tables III and IV) is shown in Figure 10 as a function of void fraction. The good agreement between the model predictions and experimental data indicates the validity of the model. One point that needs to be mentioned here is that the composition of the gypsum boards [8,11,14,15] varies from each other, which is also the reason, besides the measurement difference, that the thermal conductivity varies from each other somehow. But in this model, because of the limited information from the literature [8,11,14,15], the influence of the composition was not considered.

As introduced in the previous section, the applied heat transfer analyzer here can only be operated under 40 °C; therefore, the thermal conductivity measured in the present study at an elevated temperature only represents the microstructure change because of the dehydration reaction of the gypsum. The measured thermal conductivity of the gypsum board beyond dehydration and the experimental data from the literature are listed in Tables III and IV, respectively. As introduced before, here in the dehydrated system, only anhydrite is available, and the void fraction has also changed, which explains the variation of the measured thermal conductivity. As one can see from Table III, in the case of the same void fraction, the thermal conductivity of gypsum and dehydrated system is very different, which indicates the effect of the particle shape in the matrix on the thermal conductivity.

Table IV. Physical properties and computed initial w_0/h_0 of gypsum boards from literature [8,11,14,15] (density and thermal conductivity before and after dehydration).

Density (g/cm^3)		Initial w_0/h_0	Thermal conductivity (W/(m K))		
Room temperature	After dehydration	Ref. [26]	Room temperature	After dehydration	References
0.810	0.673	1.08	0.280	0.140	[14]
0.732	0.600	1.24	0.250	0.113	[8]
0.698	0.576	1.32	0.250	0.120	[11]
0.835	0.726	1.04	0.300	0.140	[15]
0.740	0.622	1.22	0.230	0.100	[15]
0.870	0.692	0.98	0.320	0.090	[15]

DOI: 10.1002/fam

Table V. The derived thermal physical properties of nonporous gypsum and nonporous anhydrite.

Substance	Conditions	Thermal conductivity (W/(mK))	Particle shape factor (C)	
			Computed	Ref. [27]
Anhydrite	Pure (nonporous)	0.90	1.30	1.40
Dihydrate	Pure (nonporous)	1.55	2.75	2.50

The parameters (λ_s, C, and s) in Eqs. (10) and (11) for the dehydrated system were obtained again by optimization employing the 'Solver' tool from Microsoft Excel and the experimental data (Tables III and IV), yielding 0.9 W/(mK) (λ_s), 1.3 (C), and 1% (s), respectively, for anhydrite, as listed in Table V. The obtained value for the shape factor of anhydrite is in line with that of Zehner and Schlunder [27] who reported a shape factor value of 1.40 for broken particles. This is also confirmed by the SEM analysis as shown in Figure 4(c) and 4(e). In the present study, the gypsum boards were first always heated for a full dehydration and then cooled down at ambient conditions until room temperature. A very small amount of moisture was absorbed into the gypsum boards again, which is confirmed by the small derived value of water saturation here. The derived thermal conductivity here can be understood as the thermal conductivity of pure/nonporous anhydrite. However, further research is still necessary to prove this because this is still not confirmed in literature. Finally, the thermal conductivity calculated from the model by substituting the optimized parameters (C, λ_s, and s) and the experimental data (Tables III and IV) is shown in Figure 11 as a function of void fraction. The good agreement between the model predictions and experimental data confirms the validity of the followed approach.

4. CONCLUSIONS

Gypsum boards are widely used as indoor building material because of its many advantages, such as their good thermal properties. This article addressed the thermal properties and the microstructure of gypsum board produced from β-hemihydrate through its dehydration process. The following conclusions are formulated:

1. Dehydration of gypsum occurs via two steps of first to hemihydrate and then to anhydrite according to TGA; however, these two steps are hardly distinguishable in the case of a high heating rate. The heating rate does not affect the starting dehydration temperature, but it influences the ending temperature. Study from both macroscale and microscale levels shows that given enough time, gypsum can finish the first step dehydration at 80°C and its full dehydration at 120°C.

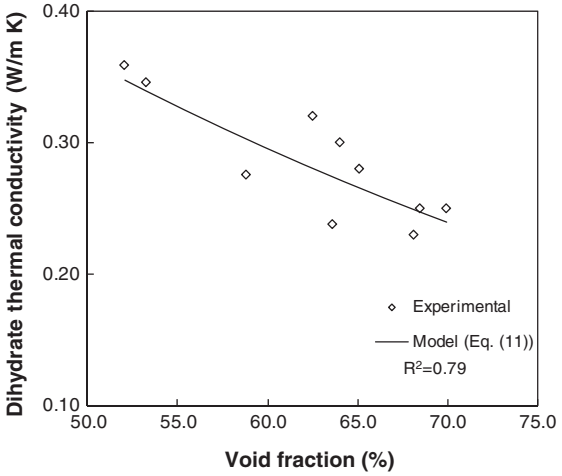

Figure 10. The thermal conductivity of gypsum boards (model predictions versus experimental data (from own tests and Refs. [8,11,14,15])).

DOI: 10.1002/fam

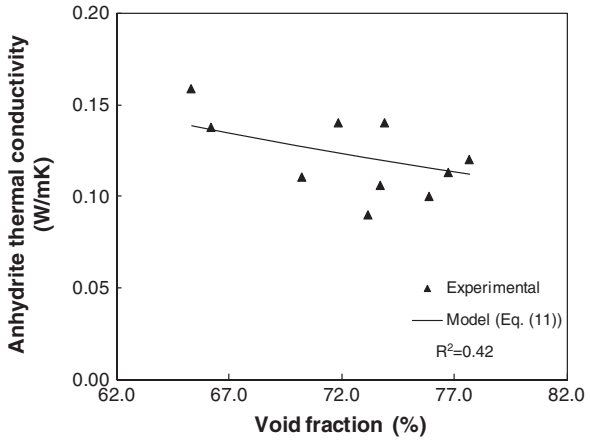

Figure 11. The thermal conductivity of dehydrated gypsum boards (model predictions versus experimental data (from own tests and Refs. [8,11,14,15])).

2. A model was proposed to describe the void fraction of the dehydrated gypsum, and it was validated by both present experiments and values taken from the literature.
3. Microstructure of the gypsum system experiences a considerable change beyond dehydration. The regularly formed gypsum crystals changed to broken particles, which consequently leads to a reduced mechanical property of the dehydrated system.
4. A link between the volumetric specific heat capacity of the gypsum boards and the initial water content was found. A model was derived to describe the thermal conductivity of the gypsum boards and the void fraction, considering both the particle shape and the free moisture in the system, and it was validated by experiments.
5. The change of the thermal properties of gypsum board was caused not only by the void fraction but also considerably by the particle shape in the system. A thermal conductivity value and a particle shape factor (C) were derived for both nonporous dihydrate and nonporous anhydrite. Also, the derived particle shape factor is in line with SEM observations and values presented by Zehner and Schlunder [27].

ACKNOWLEDGEMENTS

The authors wish to express their appreciations to Prof. Dr. H.U. Hummel and Mrs. K. Engelhardt from Knauf Gips KG (Germany) for the material supply. They furthermore express their gratitude to the European Commission (I-SSB Project, Proposal No. 026661-2) for funding this research, as well as to the following sponsors: Bouwdienst Rijkswaterstaat, Graniet-Import Benelux, Kijlstra Betonmortel, Struyk Verwo, Attero, Enci, Provincie Overijssel, Rijkswaterstaat Directie Zeeland, A&G Maasvlakte, BTE, Alvon Bouwsystemen, V.d. Bosch Beton, Selor, Twee "R" Recycling, GMB, Schenk Concrete Consultancy, Intron, Geochem Research, Icopal, BN International, APP All Remove, and Consensor (chronological order of joining). Thanks are also given to A.C.J. de Korte, P. Spiesz, M.V.A. Marinescu, A. Lazaro Garcia, and G. Quercia Bianchi.

REFERENCES

1. Ryan JV. Study of gypsum plasters exposed to fire. *Journal of Research of the National Bureau of Standards—C. Engineering and Instrumentation* 1962; **66C**(4):373–387.
2. Wirsching F. *Calcium Sulfate*. Wiley-VCH Verlag GmbH & Co. KGaA: Weinheim, 2005; 22–24. DOI: 10.1002/14356007.a04_555.
3. Groves AW. *Gypsum and Anhydrite*. Overseas Geological Surveys, Mineral Resources Division. Her Majesty's Stationery Office: London, 1958.
4. Kuntze RA. Effect of water vapor on the formation of $CaSO_4{\cdot}2H_2O$ modifications. *Journal of Chemistry* 1965; **43**:2522–2529. DOI: 10.1139/v65-346.
5. Paulik F, Paulik J, Arnold M. Thermal decomposition of gypsum. *Thermochimica Acta* 1992; **200**:195–204. DOI: 10.1016/0040-6031(92)85115-C.
6. Deutsch Y, Nathan Y, Sarig S. Thermogravimetric evaluation of the kinetics of the gypsum–hemihydrate–soluble anhydrite transitions. *Journal of Thermal Analysis* 1994; **42**:159–174. DOI: 10.1007/BF02546998.

7. Hudson-Lamb DL, Strydom CA, Potgieter JH. The thermal dehydration of natural gypsum and pure calcium sulphate dihydrate (gypsum). *Thermochimica Acta* 1996; **282/283**:483–492. DOI: 10.1016/0040-6031(95)02819-6.
8. Mehaffey JR, Cuerrier P, Carisse G. A model for predicting heat transfer through gypsum-board/wood-stud walls exposed to fire. *Fire and Materials* 1994; **18**:297–305. DOI: 10.1002/fam.810180505.
9. Andersson L, Jansson B. *Analytical fire design with gypsum — a theoretical and experimental study*. Institute of Fire Safety Design: Lund, Sweden, 1987.
10. Thomas G. Thermal properties of gypsum plasterboard at high temperatures. *Fire and Materials* 2002; **26**:37–45. DOI: 10.1002/fam.786.
11. Sultan MA. A model for predicting heat transfer through noninsulated unloaded steel stud gypsum board wall assemblies exposed to fire. *Fire Technology* 1996; 239–259. DOI: 10.1007/BF01040217.
12. Ang CN, Wang YC. The effect of water movement on specific heat of gypsum plasterboard in heat transfer analysis under natural fire exposure. *Construction and Building Materials* 2004; **18**:505–515. DOI: 10.1016/j.conbuidmat.2004.04.003.
13. Manzello SL, Gann RG, Kukuck SR, Lenhert DB. Influence of gypsum board type (X or C) on real fire performance of partition assemblies. *Fire and Materials* 2007; **31**:425–442. DOI: 10.1002/fam.940.
14. Ghazi Wakili K, Hugi E, Wullschleger L, Frank Th. Gypsum board in fire — modeling and experimental validation. *Journal of Fire Sciences* 2007; **25**:267–282. DOI: 10.1177/0734904107072883.
15. Ghazi Wakili K, Hugi E. Four types of gypsum plaster boards and their thermophysical properties under fire condition. *Journal of Fire Sciences* 2008; **27**:27–43. DOI: 10.1177/0734904108094514.
16. Yu QL, Brouwers HJH, de Korte ACJ. Gypsum hydration: a theoretical and experimental study. In *Proceedings of 17th International Conference in Building Materials (Internationale Baustofftagung)*, Weimar, Germany, **1**, Fischer HB (ed). 2009; 783–788.
17. Barthelmes M. How to prepare a laboratory gypsum plasterboard. Knauf Gips KG, Germany, 2008, personal communication.
18. International Organization for Standardization, ISO 834-1:1999. Fire-resistance Tests—Elements of Building Construction—Part 1: General Requirements, Switzerland.
19. EN 13279-2, European Standard. Gypsum binders and gypsum plasters. CEN, 2004.
20. User's guide, ISOMET model 2104 heat transfer analyzer. Applied Precision.
21. De Korte ACJ, Brouwers HJH. Calculation of thermal conductivity of gypsum plasterboards at ambient and elevated temperature. *Fire and Materials* 2010; **34**:55–75. DOI: 10.1002/fam.1009.
22. Mastersizer 2000 user manual. Malvern Instruments Ltd., 2007; 73–74.
23. Yu QL, Brouwers HJH. Microstructure and mechanical properties of β-hemihydrate produced gypsum: an insight from its hydration process. *Construction and Building Materials* 2011; **25**:3149–3157. DOI: 10.1016/j.conbuildmat.2010.12.005.
24. Hunger M. An integral design concept for ecological self-compacting concrete. Ph.D. Thesis. Eindhoven University of Technology, Eindhoven, The Netherlands, 2010.
25. Elbeyli IY, Piskin S. Thermal dehydration kinetics of gypsum and borogypsum under non-isothermal conditions, *Chinese Journal of Chemical Eingeering* 2004; **12**:302–305.
26. Brouwers HJH. *A hydration model of Portland cement using the work of Powers and Brownyard*. Eindhoven University of Technology & Portland Cement Association. ISBN: 978-90-6814-184-9, 2011. Available on http://www.cement.org
27. Zehner P, Schlunder EU. Thermal conducvitiy of granular materials at moderate temperatures. *Chemie Ingenieur Technik* 1970; **42**(14):933–941.
28. Somerton WH, Chu SL, Keese JA. Thermal behavior of unconsolidated oil sands. *Society of Petroleum Eingineers of AIME Journal* 1974; **14**(5):513–521. DOI: 10.2118/4506-PA.
29. Horai K, Simmons G. Thermal conductivity of rock-forming minerals. *Earth and Planetary Science Letters* 1969; **6**:359–368. DOI: 10.1016/0012-821X(69)90186-1.